JOURNAL OF GUIDANCE, CONTROL, AND DYNAMICS
Vol. 15, No. 2, March-April 1992

Pulse-Width Equivalent to Pulse-Amplitude Discrete Control of Linear Systems

Franco Bernelli-Zazzera* and Paolo Mantegazza†
Politecnico di Milano, Milan 20133, Italy

This paper presents a method to translate pulse-amplitude modulated discrete controls, for which many design algorithms exist, into pulse-width modulated controls extensively used in aerospace applications. Assuming that a discrete control law is available for a linear time-invariant multivariable system, the conditions for an approximate equivalent pulse-width application of the inputs are developed. The approximation is based on pulse, i.e., amplitude · duration, intensity equivalence, and on the evaluation of an optimum firing delay that maintains, independently from the control and external input, the dynamic performances of the system, including stability. A simple numerical example on a second-order system points out the benefits and drawbacks of the method, which is then applied to a typical complex aerospace design problem, i.e., shape and pointing control of a space antenna.

I. Introduction

MODERN state space control methods afford effective techniques for designing active control laws for discrete time-invariant linear systems. These techniques make available closed-form solutions of the discrete linear regulator[1] and are all based on the assumption that the control variable is the amplitude of the input, which is supposed to be unconstrained and capable of arbitrarily varying at discrete times. For these reasons this is also known as pulse-amplitude modulation control (PAM).

There are, however, some cases in which this is not a correct model of the actuators, either because they are on/off devices or because a large value of the input would violate some restrictions required to establish the mathematical model of the system. Many aerospace applications of active control fall into one of the aforementioned categories. Typical examples of the first case cited are the cold gas microthrusters used for shape and attitude control of space structures.[2] These actuators can produce time-varying forces only if their input is modulated in time and if they are coupled in two opposite directions to allow both positive and negative control forces. Electrical thermal heaters, used in thermal control of satellites, represent an example of the second case.

In all of these cases the duration of the constant amplitude input signal should be chosen as the control variable, and the on/off switching transients of the controller should be sufficiently small with respect to the shortest system time constant. This type of control system is known as pulse-width modulation control (PWM) and is unfortunately nonlinear and difficult to design unless a suitable linearization method or sufficient conditions for the applicability of standard linear techniques are available.

Many methods exist for linear pulse-width modulation design, including the pulse-width/pulse-frequency modulation (PWPF) in which both the pulse frequency and the pulse width are variable.[3] These methods have proven very effective in many aerospace applications, but their design is generally carried out for each actuator on a single-input/single-output equivalent linearization. Thus, possible cross effects in case of multi-input systems are generally dealt with by extensive simulations in the final design phase to tune the multi-input operation.[4]

It is then worth searching for an equivalent linearization capable of directly taking into account multi-inputs, leaving to the final design refinement only the evaluation of actuator saturations and limit cycles characteristics.

A method to linearize a system with multi-input PWM actuators whose input can never be zero over an entire sampling interval, but at most have a zero average value, is presented in Ref. 5. In most cases this approach would lead to a useless waste of control power, representing a severe penalty in some applications where the available power is limited, and moreover it cannot stabilize unstable systems.

With this in mind, a new method is proposed to take into account the presence of pulse-width modulated actuators; that method has two main advantages with respect to the one presented in Ref. 5, i.e., it allows a zero input level instead of an averaged zero, and it establishes a direct connection between PWM and PAM. In this way the control law can be designed, with great computational advantage, for a linear system with PAM control and then applied in a nonlinear way to the real system.

The approach adopted in the present work consists of evaluating the response of a discrete linear time-invariant system to a PWM input and determining the error of this response with respect to that obtained with a PAM input having an equivalent impulse over the sampling period. The response error is seen to be dependent on the time delay of the impulse from the sampling instant, and it is shown that a delay for which the error is minimized always exists. Therefore, if there is no saturation, by applying an "equivalent pulse" input with a suitable delay, it is possible to achieve a good mapping of the PAM control problem into a PWM control.

The validity of this approach is illustrated on a simple second-order system and tested on an aerospace application, i.e., the design of an active shape and pointing control system for a large Shuttle-attached antenna.

II. Problem Formulation

Assuming that a discrete PAM control law for a linear time-invariant continuous system has been computed, the goal is to implement it in a PWM mode. The system dynamics are governed by a linear system of differential equations

$$\{\dot{x}\} = [A]\{x\} + [B]\{u\}, \qquad \{y\} = [C]\{x\} \tag{1}$$

where $\{x\}$, $\{u\}$, and $\{y\}$ are the k states, m inputs, and n outputs of the system, and $[A]$, $[B]$, and $[C]$ are matrices of appropriate dimensions. In the PAM control formulation, the input $\{u\}$ is supposed to be constant over the sampling period

Received June 21, 1990; revision received Oct. 5, 1990; accepted for publication Oct. 24, 1990.

*Ph.D., Fellow of Ing. P. Foresio Foundation, Department of Aerospace Engineering, Via Golgi 40.

†Professor, Department of Aerospace Engineering, Via Golgi 40.

Δ and with no delays from the sampling instant t,[1] whereas in PWM mode the amplitude $\{u_M\}$ is fixed and the unknowns become the fraction of time δ during which the controller is active and the delay τ from the sampling instant (see Fig. 1). In this approach, the pulse-width control is therefore suitable only for discrete controls and has no equivalent in continuous control systems.

Superimposing the effects of each input, the response of the system subject to the PAM input is[1,6]

$$\{x(t+\Delta)\} = [e^{A\Delta}]\{x(t)\} + \sum_{i=1}^{m} [\Psi(\Delta)]\{B_i\}u_i\Delta \tag{2}$$

having introduced the notation

$$[\Psi(d)] = \sum_{i=0}^{\infty} \frac{[A]^i}{(n+1)!}\, d^i \tag{3}$$

It is required to obtain the same response with a PWM input.

Response to a Pulse-Width Control Input

Referring to the pulsed input depicted in Fig. 1, the response of the system is

$$\{x(t+\Delta)\} = [e^{A\Delta}]\{x(t)\} + \sum_{i=1}^{m} [e^{A(\Delta-\tau)}][\Psi(-\delta)]\{B_i\}u_{Mi}\delta_i \tag{4}$$

Since the system is linear, the effects of each input can be superimposed, so that a single input system will be hereafter considered.

Supposing that the PAM input is transformed into a PWM input with an equivalent pulse over the sampling period, i.e.,

$$\delta = u\Delta/u_M \tag{5}$$

and that δ is small enough to allow the approximation

$$[e^{-A\delta}] = [I] - [A]\delta \tag{6}$$

the response of Eq. (4) becomes

$$\{x(t+\Delta)\} = [e^{A\Delta}]\{x(t)\} + [e^{A(\Delta-\tau)}]\{B\}u_M\delta \tag{7}$$

Comparison of Eq. (7) with Eq. (2) shows no differences in the state transition matrix but major differences in the input term. This is to be expected since the unforced dynamics of the system cannot be changed by a modification of the input.

Recalling the expression of the matrix exponential and Eq. (5), the error vector between the desired dynamics, i.e., Eq. (2), and the actual dynamics, i.e., Eq. (7), is

$$\{E\} = -\sum_{k=1}^{\infty} \frac{[A]^k[(k+1)(\Delta-\tau)^k - \Delta^k]\{B\}u\Delta}{(k+1)!}$$

$$= -\sum_{k=1}^{\infty} \frac{[A]^k[(k+1)(\Delta-\tau)^k - \Delta^k]\{B\}u_m\delta}{(k+1)!} = \{\epsilon\}u_M\delta \tag{8}$$

This error is proportional to the integral of the input over the sampling period, the coefficient vector of proportionality

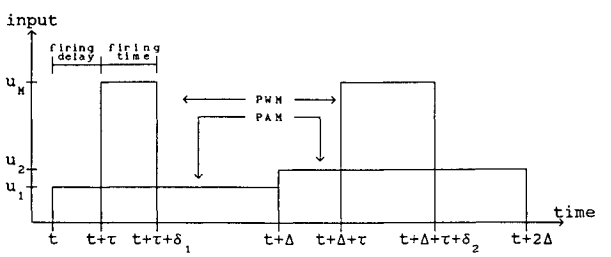

Fig. 1 Illustration of discrete (PAM) and equivalent pulse-width (PWM) inputs.

$\{\epsilon\}$ being a function of the firing delay τ and of the system matrices $[A]$ and $[B]$. It appears therefore reasonable to look for a particular delay $\bar{\tau}$ for which $\{\epsilon\}$ is minimized while keeping the approximation of a small δ. Some very simple considerations allow the conclusion that $\bar{\tau}$ always exists. In fact, when $\{\epsilon\}$ is computed for three particular values of τ, precisely $\tau = 0$ (PWM fired at the beginning of the sampling interval), $\tau = \Delta - \delta$ (PWM fired at the end of the sampling interval), and $\tau = \Delta/2$, it becomes

$$\tau = 0 \rightarrow \{\epsilon\} = -\sum_{k=1}^{\infty} \frac{k[A]^k\Delta^k\{B\}}{(k+1)!} \tag{9}$$

$$\tau = \Delta - \delta \rightarrow \{\epsilon\} = -\sum_{k=1}^{\infty} \frac{[A]^k[(k+1)(\delta\Delta)^k - \Delta^k]\{B\}}{(k+1)!}$$

$$\cong +\sum_{k=1}^{\infty} \frac{[A]^k\Delta^k\{B\}}{(k+1)!} \tag{10}$$

$$\tau = \Delta/2 \rightarrow \{\epsilon\} = -\sum_{k=2}^{\infty} \frac{[A]^k[(k+1)(\Delta/2)^k - \Delta^k]\{B\}}{(k+1)!} \tag{11}$$

Therefore, from Eqs. (9) and (10) it is clear that the error vector reverses its sign as the firing delay grows from 0 to $\Delta - \delta$. In particular, for $\tau = \Delta/2$, the first term of the series becomes zero. The delay $\bar{\tau}$ can thus be approximated by $\bar{\tau} = (\Delta/2) + \tilde{\tau}$, with $\tilde{\tau}$ computed by minimizing the norm of the error. Indicating by $/\tau$ the derivative with respect to τ, evaluating the derivatives at $\tau = \Delta/2$, and introducing the notation

$$[\theta] = [e^{A\Delta/2}], \qquad [\Xi] = [\Psi(\Delta)] \tag{12}$$

$$\{\epsilon\}_{\tau=\Delta/2} = \{\mathcal{E}\} = [\Xi - \theta]\{B\} \tag{13}$$

we obtain

$$\tilde{\tau}[(\{\epsilon\}'\{\epsilon\})_{/\tau}]_{\tau=\Delta/2} = -\{\mathcal{E}\}'\{\mathcal{E}\} \tag{14}$$

with

$$\{\mathcal{E}\}'\{\mathcal{E}\} = \{B\}'[\Xi - \theta]'[\Xi - \theta]\{B\} \tag{15}$$

$$[(\{\epsilon\}'\{\epsilon\})_{/\tau}]_{\tau=\Delta/2} = \{B\}'([\theta]'[A]'[\Xi - \theta] + [\Xi - \theta]'[A][\theta])\{B\} \tag{16}$$

so that

$$\tilde{\tau} = -\frac{\{B\}'[\Xi - \theta]'[\Xi - \theta]\{B\}}{\{B\}'([\theta]'[A]'[\Xi - \theta] + [\Xi - \theta]'[A][\theta])\{B\}} \tag{17a}$$

$$\bar{\tau} = \frac{\Delta}{2} - \frac{\{B\}'[\Xi - \theta]'[\Xi - \theta]\{B\}}{\{B\}'([\theta]'[A]'[\Xi - \theta] + [\Xi - \theta]'[A][\theta])\{B\}} \tag{17b}$$

In this approximation, the optimum firing delay $\bar{\tau}$ for each input can thus be evaluated independently from the control law and the input u_M. In fact, it depends only on the system matrices $[A]$ and $[B]$, and on matrices $[\Xi]$ and $[\theta]$, that are in turn related only to Δ. This technique converts a PAM into a PWM control, leaving the dynamic behavior and the stability of the controlled system unaffected. It is then possible to compute the control law by analyzing the PAM system, which is linear.

Response to a Reference Command

The behavior of the system represented by Eq. (1) subject to a reference command u_c will now be evaluated by determining the equivalent pulse-width firing time δ_c.

The response of the discrete system to a reference command u_c is

$$\{x(t+\Delta)\} = [e^{A\Delta}]\{x(t)\} + [\Psi(\Delta)]\{B\}u_c\Delta \tag{18}$$

At steady state we have

$$\{x(t+\Delta)\} = \{x(t)\} = \{x_s\} = -[A]^{-1}\{B\}u_c \tag{19}$$

If the input includes both a reference command and a control input the response becomes

$$\{x(t+\Delta)\} = [e^{A\Delta}]\{x(t)\} + [\Psi(\Delta)]\{B\}(u+u_c)\Delta \tag{20}$$

Transforming u into δ according to Eq. (5) and u_c into a yet unknown δ_c, and applying the constant input u_M for a time $\delta+\delta_c$, with a delay τ, supposing δ small, we obtain

$$\{x(t+\Delta)\} = [e^{A\Delta}]\{x(t)\} + [e^{A(\Delta-\tau)}][e^{-A\delta_c}]\{B\}u_M\delta + [e^{A(\Delta-\tau)}][\Psi(-\delta_c)]\{B\}u_M\delta_c \tag{21}$$

At the steady-state conditions $\delta = 0$, and it is desired to obtain $\{x(t+\Delta)\} = \{x(t)\}$, so that

$$([e^{A\Delta}] - [I])\{x(t)\} = -[e^{A(\Delta-\tau)}][\Psi(-\delta_c)]\{B\}u_M\delta_c \tag{22}$$

With a PWM reference command, the state vector cannot be made constant over the sampling period even in steady-state conditions. It is desirable, however, for the equivalence to the discrete command, that the average value $\{\bar{x}\}$ over the sampling period approaches $\{x_s\}$, the value of the continuous steady-state response to a constant input, as much as possible. The average value $\{\bar{x}\}$ is

$$\{\bar{x}\} = \frac{1}{\Delta}\int_0^{\Delta}\{x(t+\lambda)\}\,d\lambda \tag{23}$$

where the vector $\{x(t+\lambda)\}$ assumes different values depending on λ, and precisely

$$[e^{A\lambda}]\{x(t)\} \quad \text{for} \quad 0<\lambda\le\tau \tag{24a}$$

$$[e^{A\lambda}]\{x(t)\} + [e^{A(\lambda-\tau)}][\Psi(\tau-\lambda)] \times \{B\}u_M(\tau-\lambda) \quad \text{for} \quad \tau<\lambda\le\tau+\delta_c \tag{24b}$$

$$[e^{A\lambda}]\{x(t)\} + [e^{A(\lambda-\tau)}][\Psi(-\delta_c)] \times \{B\}u_M\delta_c \quad \text{for} \quad \tau+\delta_c<\lambda\le\Delta \tag{24c}$$

Evaluating the integral we have

$$\{\bar{x}\} = \frac{1}{\Delta}[A]^{-1}([e^{A(\Delta-\tau)}][\Psi(\delta_c)]\{B\}u_M\delta_c - \{B\}u_M\delta_c + ([e^{A\Delta}] - [I])\{x(t)\}) \tag{25}$$

By virtue of Eq. (22), Eq. (25) becomes

$$\{\bar{x}\} = -\frac{1}{\Delta}[A]^{-1}\{B\}u_M\delta_c \tag{26}$$

Therefore, comparing Eq. (26) with Eq. (19), it is seen that to have $\{\bar{x}\} = \{x_s\}$, the discrete command u_c has to be transformed, regardless of the firing delay τ, into a pulsed command of firing duration

$$\delta_c = u_c\Delta/u_M \tag{27}$$

This should have been expected since, if a steady-state condition is reached, the effect of different delays would simply be a time shift of the response peaks, with no effect on the integral of the response over a sampling interval.

Closed-Loop Stability Analysis

The most important point in designing an active control system is to ensure the closed-loop stability of the system. Supposing a constant gain output feedback control law of the kind

$$\{u\} = [K][C]\{x(t)\} \tag{28}$$

the closed-loop response of the system subject to a PAM control input is

$$\{x(t+\Delta)\} = ([\Phi] + [\Gamma][K][C])\{x(t)\} = [N_{\text{PAM}}]\{x(t)\} \tag{29}$$

where

$$[\Phi] = [e^{A\Delta}], \qquad [\Gamma] = [\Psi(\Delta)][B]\Delta \tag{30}$$

Vice versa, the closed-loop response of the same system subject to a PWM control input defined by Eqs. (5) and (6) and applied with an arbitrary firing delay τ is given by

$$\{x(t+\Delta)\} = ([\Phi] + [e^{A(\Delta-\tau)}][B][K][C]\Delta)\{x(t)\} = [N_{\text{PWM}}]\{x(t)\} \tag{31}$$

If the delay τ is computed according to Eq. (17b), then, due to the assumptions made to compute $\bar{\tau}$, the following relations hold

$$[e^{A(\Delta-\bar{\tau})}B]\cdot u_M\delta = [\Gamma]\cdot u \tag{32a}$$

$$[e^{A(\Delta-\bar{\tau})}B\Delta] = [\Gamma] \tag{32b}$$

$$[N_{\text{PWM}}] = [N_{\text{PAM}}] \tag{32c}$$

and therefore the closed-loop stability properties of the PAM controlled system apply also to PWM, either for open-loop stable or unstable systems. This allows the computation of the feedback gain matrix $[K]$ by referring to a PAM system. This fact has a great computational advantage since many theoretical studies and numerical algorithms are available for this purpose.

For any other value of the firing delay τ, the closed-loop stability of the discretely controlled system does not automatically guarantee the stability of the pulse-width controlled system. In fact, if the actual delay is $\tau = \bar{\tau} + \xi$, the relation between the closed-loop state matrix of the PWM and PAM controlled system is given by

$$[N_{\text{PWM}}]_{(\tau=\bar{\tau}+\xi)} = [N_{\text{PAM}}] + ([e^{A\xi}] - [I])[\Gamma][K][C] \tag{33}$$

and the eigenvalues of the matrix $[N_{\text{PWM}}]$ can differ substantially from those of $[N_{\text{PAM}}]$.

This obviously holds only if no control saturations occur. In PWM control the input gets saturated if δ becomes greater than the sampling time Δ, a condition equivalent to the amplitude saturation of the discrete case.

III. Numerical Examples

To validate the theory, two different control designs are presented, i.e., a spring-mass-damper system and a shape and pointing control system for a space antenna. The active controller has been determined in both cases by means of a discrete linear suboptimal control technique,[7] and the system response has then been evaluated via an exact nonlinear integration of the equations of motion, to take into account the presence of saturations and PWM actuators.

Pulse-width modulated actuators are always assumed to be coupled and acting in opposite directions, the switching between the two being determined by the sign of the firing duration time δ.

Example 1: Second-Order System

The first test was carried out to demonstrate the effects of the firing delay τ, the maximum input amplitude u_M, and the

sampling time Δ on the transient and steady-state response of a system subjected to a control input and to a reference command by using the spring-mass-damper system shown in Fig. 2. The dynamics of the system having mass m, damping coefficient c, and elastic spring constant k is represented in the state-space form by

$$\begin{Bmatrix} \ddot{x} \\ \dot{x} \end{Bmatrix} = \begin{bmatrix} -2\zeta\omega & -\omega^2 \\ 1 & 0 \end{bmatrix} \begin{Bmatrix} \dot{x} \\ x \end{Bmatrix} + \begin{bmatrix} 1/m \\ 0 \end{bmatrix} \{f\} \tag{34}$$

the input force $\{f\}$ is given by

$$\{f\} = k_v\{\dot{x}\} + k_e\{x-r\} + m\omega^2\{r\} \tag{35}$$

where $\{r\}$ is the desired set point. It can be noted that the feed-forward control, i.e., $m\omega^2\{r\}$, is capable of achieving the desired set point in case of perfect model knowledge. Thus the feedback terms are added to improve response performances and to take into account uncertainties in the model knowledge.

The system parameters are $m = 1$, $\zeta = 0.1$, and $\omega = 6.28$, i.e., an open-loop natural frequency of 1 Hz. With these system characteristics, a controller sampling time of 0.1 s appears appropriate. Specifications for the closed-loop system are established in terms of damping factor, to be as close as possible to 0.7, and a sufficiently low input requirement to prevent undesirable control saturations in PWM operational mode. To meet the dynamic performances, k_v and k_e are computed for a PAM control by minimizing the discrete quadratic performance index[7]:

$$J = E\left\{ \sum_{n=1}^{\infty} (\{y\}_n^T[Q_y]\{y\}_n + \{f\}_n^T[Q_u]\{f\}_n) \right\} \tag{36}$$

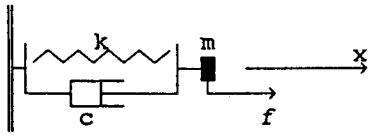

Fig. 2 Second-order system.

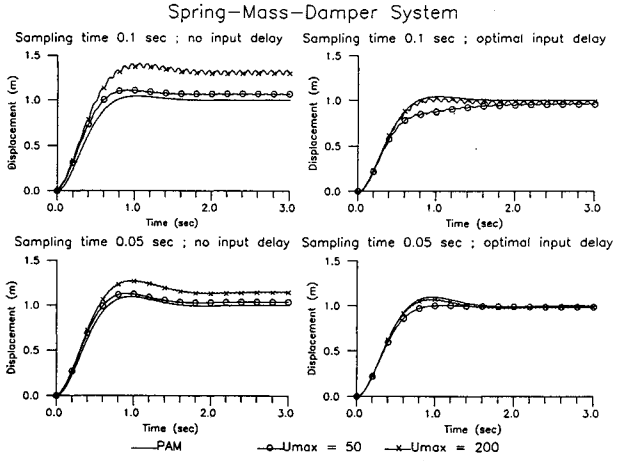

Fig. 3 Displacement response of second-order system (PAM and PWM).

Table 1 Closed-loop eigenvalues and optimal firing delays of second-order system

Δ, s	$\bar{\tau}$, s	ω, rad/s	ζ	k_v	k_e
0.1	0.0477	4.35	0.71	− 2.67	24.2
0.05	0.0241	4.08	0.60	− 2.67	24.2

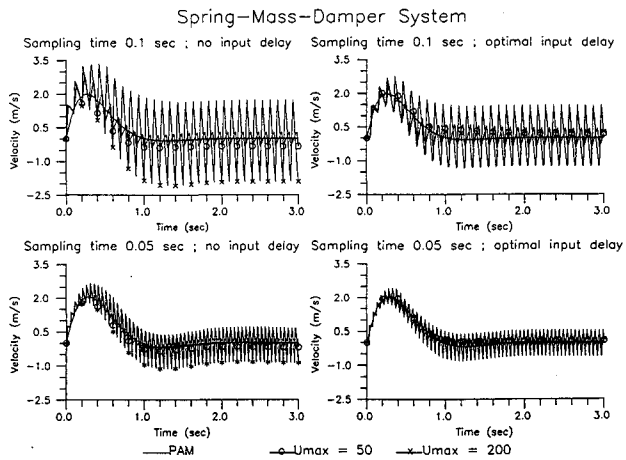

Fig. 4 Velocity response of second-order system (PAM and PWM).

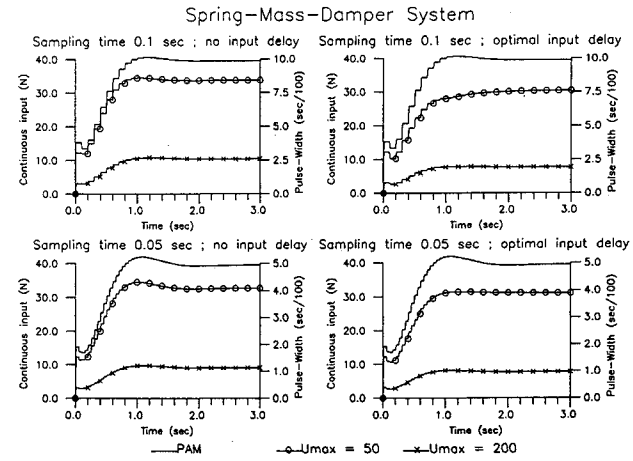

Fig. 5 Inputs to second-order system (PAM and PWM).

where $E\{\cdot\}$ indicates the expected value operator for a suitable set of stochastic disturbances and/or nonzero initial conditions, and

$$\{y\} = [\dot{x} \quad \{x-r\}]^T \tag{37a}$$

$$[Q_y] = \begin{bmatrix} 20 & 0 \\ 0 & 1 \end{bmatrix} \tag{37b}$$

$$[Q_u] = [0.1] \tag{37c}$$

which leads to $k_v = -2.67$, $k_e = 24.2$.

Two different sampling times were then used to analyze the system response, namely $\Delta = 0.1$ and 0.05 s. Shorter sampling times are not considered since this would mean operating almost as in continuous time, so that PWM control would not be applicable. The optimal firing delay $\bar{\tau}$ and the closed-loop eigenvalues are collected in Table 1, whereas the step responses to a unit reference command, either PAM or PWM, with different delays and maximum amplitudes, are reported in Figs. 3–5.

In Fig. 5 the PAM input is plotted vs the left ordinate axis, whereas PWM inputs, i.e., duration, are plotted vs the right ordinate axis.

Considering Table 1, it should be immediately remarked that, depending on Δ, the system eigenvalues are not constant. This is not surprising since, because of Eq. (30), both the state transition matrix $[\Phi]$ and input matrix $[\Gamma]$ depend on Δ, whereas in this particular case $[K]$ and $[C]$ are held constant. For the purpose of the present example, this is not important, since the comparisons are done between PAM and PWM responses of analogous systems, with the sampling period as the distinctive parameter of the system configuration.

The analysis of the step responses is in good agreement with the theoretical analysis. A few considerations should be noted.

As stated in Eq. (8), if the delay is not optimal, the error of the PWM controlled response relative to the "desired" response, i.e., the PAM controlled response, is proportional to the input amplitude u_M, and this clearly appears from the steady-state biases in Figs. 3 and 4. Moreover, in this particular example, the value $u_M = 50$ is quite close to the steady-state discrete input, which is precisely 39.48. Then it is obvious that the steady-state value of δ will be quite close to Δ. This does not agree with the assumptions made to establish the relationship between PAM and PWM control and explains why the performances of the system subjected to a PAM input and to a PWM input with null delay are quite similar. In fact, from Eq. (4), it is seen that, for $\delta = \Delta$, the equivalence between PAM and PWM control is obtained with $\tau = 0$.

Figures 3 and 4 clearly point out the peculiar response of PWM controlled systems. Even at "steady state," the system tends to oscillate around the average condition, due to the on/off input type, and the only reduction in amplitude is due to the integral action of the system dynamics. From Fig. 5 it can be seen that the PWM is always of the same sign. Thus the limit cycles are due only to the elastic action of the system and not to a change of sign of the control force. This fact also explains why the limit cycle amplitude is larger for the higher input level. In fact, since the pulse intensity is equivalent, the duration is shorter for the higher input, and thus it leaves more time for the elastic action to operate, causing a larger amplitude oscillation. The optimum firing delay τ guarantees that the steady-state response of the PAM and PWM controlled systems are the same. The difference in the transient response depends on the input amplitude. Higher amplitudes mean smaller pulse firing durations δ, and so the approximation of Eq. (6) becomes indeed true, and Eq. (7) represents the real dynamic behavior of the system, so that the optimal firing delay effectively minimizes the response error. The same holds also for smaller sampling periods since, as shown by Eq. (5), δ is also proportional to Δ.

Considering that in discrete control the sampling time is usually limited by the control hardware and cannot therefore be made as small as possible, it can then be stated that it is advisable to select the optimal firing delay for PWM control and, compatible with actuator limits, operate with a sufficiently high input level.

Example 2: Shuttle-Attached Antenna

The second example shows an application of a mixed PAM/PWM control to the shape and pointing control of a large space antenna. This system is clearly more complex than the preceding one, and since the antenna structural damping is neglected and the overall system is a free body, it is open-loop neutrally stable. Nevertheless, it will be shown that the equivalent PWM control can be successfully applied also to this kind of system.

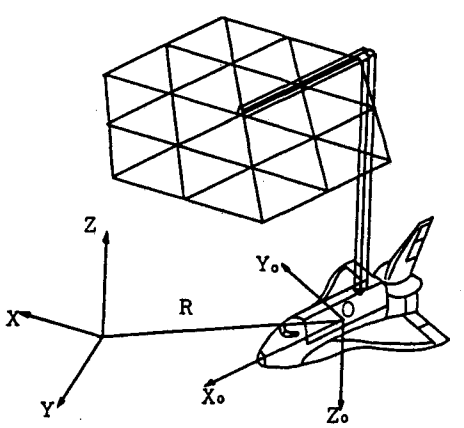

Fig. 6 Topology of the Shuttle-attached antenna.

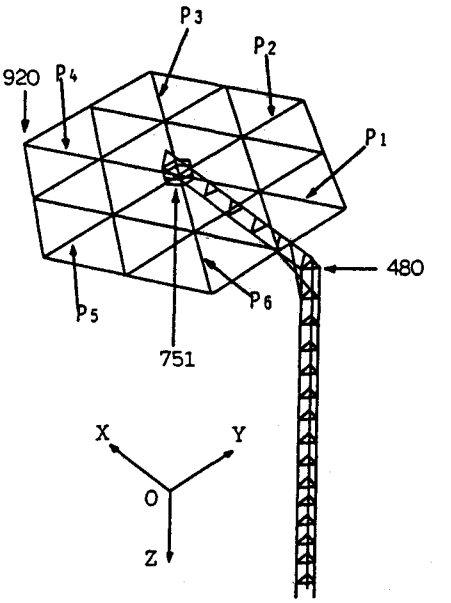

Fig. 7 Finite element model of the antenna and location of piezoelectric actuators.

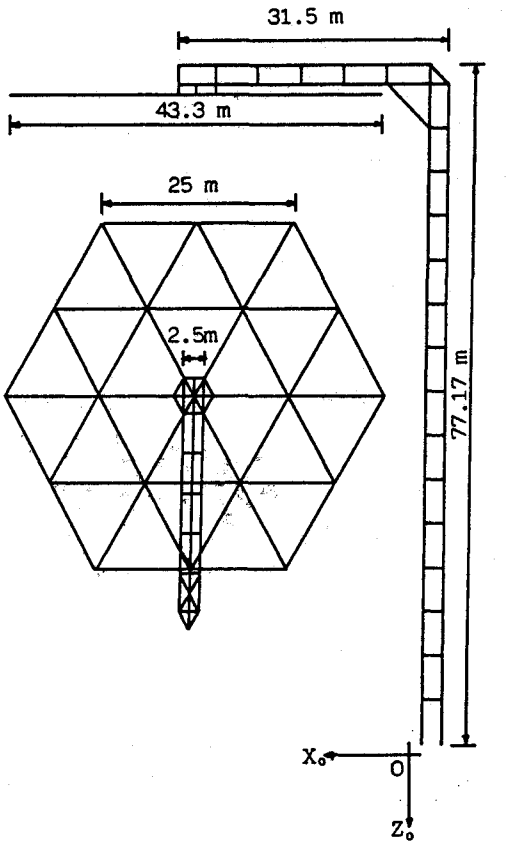

Fig. 8 Dimensions of the antenna.

The antenna studied in the present work consists of a large dish connected to the Shuttle by an aluminum L-shaped flexible truss.[8] Figures 6–8 depict the topology and dimensions of the antenna, along with its finite element representation consisting of 95 grid points. Three representative points are marked in Fig. 7, and their dynamic behavior will be used to assess the performance of the system, i.e., node 480 at the corner of the flexible truss, node 751 at the center of the dish, and node 920 on the dish boundary. The flexible truss is considered to be clamped to the Shuttle. All of the elements are supposed to be uniform tubular beams with a cross-sectional area of 200 mm^2, Young's modulus equal to 72,520

N/mm^2, and density 3000 kg/mm^3. The total mass of the antenna is 635 kg, and the total system mass is 102,788 kg.

The system dynamics are governed by two sets of equations, one governing the average rigid body motion and another governing the small perturbations of the rigid motion and the elastic deformations. A detailed derivation of the equations of motion is found in the literature[9,10] and will not be repeated here for the sake of conciseness. Instead, attention is focused on the small perturbed overall motion and on the elastic deformations as represented by the simplified system

$$\begin{cases} [m]\{\ddot{R}_1\} + [\Lambda][V]\{\ddot{q}\} = \{F_1\} \\ [I_o]\{\ddot{\beta}\} + [\Sigma]'[V]\{\ddot{q}\} = \{M_1\} \\ [V]'[\Lambda]'\{\ddot{R}_1\} + [V]'[\Sigma]\{\ddot{\beta}\} + \{\ddot{q}\} + [\lambda^2]\{q\} \\ \quad = [V]'\{Q_1\} \end{cases} \tag{38}$$

in which only two coupling terms $[\Lambda]$ and $[\Sigma]$ are present. In Eq. (38), $[V]$ is the matrix of the antenna branch modes, i.e., the modes of the antenna clamped to the still standing Shuttle; $[I_o]$ and $[m]$ are the inertia and mass matrices of the system in the undeformed condition; $\{R\}$, $\{\beta\}$, and $\{q\}$ are, respectively, the perturbed displacement and orientation of the system center of gravity and the antenna branch modal coordinates.

It is possible to reformulate Eq. (38) as a set of first-order linear differential equations, with state vector $\{x\}$, state matrix $[A]$, input vector $\{u\}$, and input matrix $[B]$ given by

$$\{\dot{x}\} = [A]\{x\} + [B]\{u\} \tag{39a}$$

$$\{x\} + [\dot{R}_1\ \dot{\beta}\ \dot{q}\ R_1\ \beta\ q]', \qquad \{u\} = [F_1\ M_1\ V'Q_1]' \tag{39b}$$

$$[A] = \begin{bmatrix} 0 & -M^{-1}K \\ I & 0 \end{bmatrix}, \qquad [B] = \begin{bmatrix} M^{-1} \\ 0 \end{bmatrix} \tag{39c}$$

$$[M] = \begin{bmatrix} m & 0 & \Lambda V \\ 0 & I_o & \Sigma' V \\ V'\Lambda & V'\Sigma & I \end{bmatrix}, \qquad [K] = \begin{bmatrix} 0 & 0 & 0 \\ 0 & 0 & 0 \\ 0 & 0 & \lambda^2 \end{bmatrix} \tag{39d}$$

The branch mode shapes corresponding to the lowest 10 eigenfrequencies were used to represent the antenna. This restricted choice of natural mode shapes is considered accurate enough since, as illustrated in Table 2, they are representative of a wide class of possible motions of the antenna. The analysis of the eigenvalues of the $[A]$ matrix of Eq. (39), also reported in Table 2, shows that basically the coupling has the effect of modifying the flexible branch modes that nonetheless are enough to correctly represent the lowest vibration modes of the whole system since, due to the massive Shuttle, the last branch modes are practically the vibration modes.

Table 2 Branch mode shapes of the clamped and Shuttle-attached antenna

Mode	Clamped frequency, rad/s	Mode shape	Shuttle-attached frequency, rad/s
1	8.05e − 3	Short truss bending	1.04e − 2
2	3.75e − 2	Dish rotation about X axis	3.76e − 2
3	9.56e − 2	Long truss bending	9.73e − 2
4	9.74e − 2	Dish rotation about Y axis	1.08e − 1
5	1.11e − 1	Dish cupping	1.12e − 1
6	1.12e − 1	Long truss twist	1.41e − 1
7	1.83e − 1	Dish bending	1.83e − 1
8	1.84e − 1	Dish bending	1.84e − 1
9	2.55e − 1	Dish torsion and long truss twist	2.68e − 1
10	3.47e − 1	Dish torsion and warping	3.47e − 1

The control system consists of 23 actuators driven in a decentralized way from collocated sensors. Six of them exert forces and moments on all six degrees of freedom of the rigid Shuttle; eight thrusters are placed on the flexible truss: four on the truss corner acting in the X and Y directions and four at the end acting in the Y and Z directions. The corresponding sensors are local displacement and velocity sensors. The control of the dish is carried out by using three reaction wheels, acting along the three axes at the connection with the truss, driven by angle and angular rate sensors and by six piezoelectric layers on the dish's outer radial beams, marked in Fig. 7 as P_1-P_6. The piezoelectric layers are supposed to work in couples, one acting as an actuator and one as a sensor, measuring local deformations. For the piezoelectric actuators a lead-lag network has also been devised to provide better performance.

Let $\{u_s\}$ indicate the forces acting on the Shuttle, $\{u_t\}$ the PWM forces on the truss, $\{u_d\}$ the moments applied at the dish center, and $\{u_p\}$ the forces exerted by the piezoelectric actuators; by partitioning the measurements vector accordingly, the decentralized feedback control law can be expressed as

$$\{u_s\} = [K_s]\{m_s\} + [K_s]\{m_s\} \tag{40a}$$

$$\{u_t\} = [K_t]\{m_t\} + [K_t]\{m_t\} \tag{40b}$$

$$\{u_d\} = [K_d]\{m_d\} + [K_d]\{m_d\} \tag{40c}$$

$$\{u_p\} = [K_p(s + b)/(s + a)]\{m_p\} \tag{40d}$$

The most common performance indexes used for antennas are the nominal pointing error and the average shape error, whose definitions and limits for a large reflector are

$$\text{pointing error} = \sqrt{\{\vartheta_c\}'\{\vartheta_c\}/3} < 0.02 \text{ deg} \tag{41a}$$

$$\text{shape error} = \sqrt{\{z_a\}'\{z_a\}/n_a} < 5 \text{ mm} \tag{41b}$$

where $\{\vartheta_c\}$ represents the three rotations at the center of the antenna, and $\{z_a\}$ are the displacements of the n_a nodes of the dish perpendicular to the dish plane. These performance indexes are nonlinear and difficult to treat numerically, so a more simple linear quadratic function of a performance vector $\{\chi\}$ is used to build a suitable quadratic cost function to be minimized

$$\{\chi\} = [(\dot{R}_{1x} + \dot{R}_{1y} + \dot{R}_{1z} + R_{1x} + R_{1y} + R_{1z}) \\ (\dot{\beta}_1 + \dot{\beta}_2 + \dot{\beta}_3 + \beta_1 + \beta_2 + \beta_3)\ q]' \tag{42}$$

$$J = \int (\{\chi\}'[Q_x]\{\chi\} + \{u\}'[Q_u]\{u\})\ dt \tag{43}$$

The matrices $[Q_x]$ and $[Q_u]$ are diagonal with unit weighting factors for the first two entries of the performance vector, 10 for the modal coordinates, 1/10 for the Shuttle actuators, 1/1000 for the truss actuators, and 1/10,000 for the piezoelectric actuators.

A sampling rate of 2 samplings/s, i.e., 10 times the highest natural frequency considered, was chosen for the controller.

Table 3 reports the optimal firing delays for each of the four pairs of thrusters located on the flexible truss. As predicted by

Table 3 Actuator firing delay times of the Shuttle antenna system

Actuator	Delay τ
F_x480	0.2497
F_y480	0.2485
F_y751	0.2495
F_z751	0.2496

Table 4 Gain parameters and lead and lag constants of the piezoelectric actuators

Actuator	K_p	b	a
P_1	−314.4	0.8095	0.5396
P_2	151.9	1.276	0.7791
P_3	−115.2	0.0185	0.0084
P_4	−219.6	0.0226	0.2780
P_5	161.5	1.125	0.5446
P_6	−309.1	0.2713	0.3213

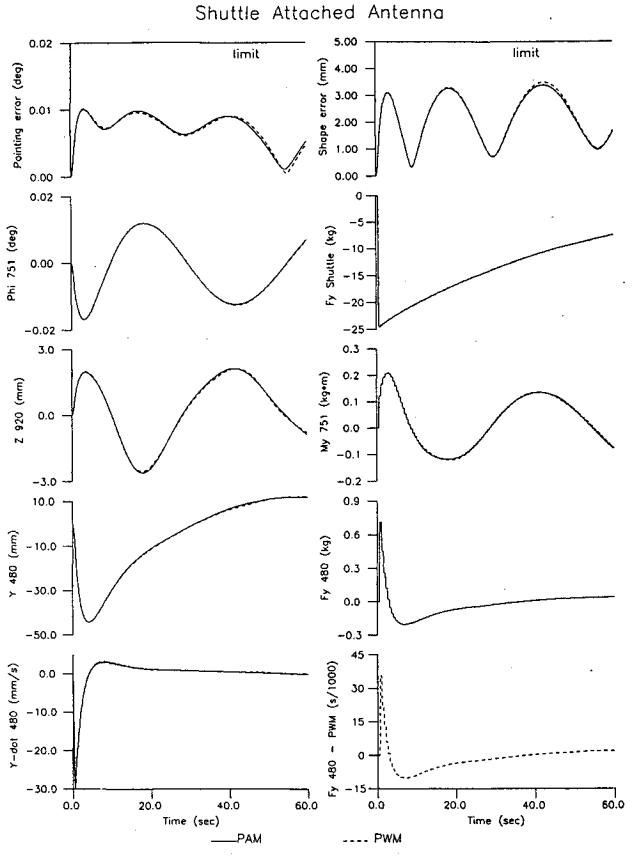

Fig. 9 Impulse response of the Shuttle-antenna system.

Eq. (17), the optimal delays are quite close to half the sampling period.

An analysis of the gain parameters, lead and lag constants of the piezoelectric actuators reported in Table 4, shows a nonsymmetric behavior of the control, in spite of the structural symmetry, due to the unsymmetry of the natural modes representative of the antenna. A mixture of integrating and derivative effects of the lead-lag networks can be seen, and it is remarked that this solution is the best one compatibly with the structure of the system, since the lead and lag constants were included as unknown parameters during the minimization process.

The closed-loop response of the system to an impulse comparable to the effect of a lateral docking maneuver, producing a lateral velocity increment of the Shuttle of 1 cm/s in the Y direction, has been simulated considering PAM and PWM control of the truss. In the latter case all of the thrusters are supposed to have a unique thrust level of 10 kg. The time histories reported in Fig. 9 are in good agreement with the performances already discussed.

The sampling time and the amplitude of the PWM inputs are well within the hypothesis at the base of the theory presented. No control saturations occur, and once more it is demonstrated that the application of PWM with an optimal delay is perfectly equivalent to PAM control. It is remarked that this system is open-loop neutrally stable, and despite this fact the response of the PWM controlled system shows no tendency to become unstable and no errors in the system displacements or discrete inputs. This holds both for points located near and far from the location of the pulsed thrusters. Just a slight intersample ripple appears in the velocity at the truss corner where the pulsed actuator is located.

IV. Conclusions

A method for the pulse-width application of a discrete pulse amplitude control law computed for a linear system has been proposed. This conversion technique maintains the dynamic performance of the PAM control and requires a simple equivalence of the total impulse applied during each sampling interval and the computation of the firing time delay. Since the latter depends only on system parameters, it can be computed separately from the control law. This fact is fairly attractive for practical applications in which a PWM control is required, since it allows computation of the control law for a PAM control system, using one of the many available software packages. The only further operation required to perform the conversion from PAM to PWM is one multiplication for each of the inputs and a constant firing delay which, under reasonable assumptions, does not cause unpredictable effects on the system performance.

References

[1]Franklin, G. F., and Powell, J. D., *Digital Control of Dynamic Systems,* Addison-Wesley, Reading, MA, 1980.

[2]Sutton, G. P., *Rocket Propulsion Elements: An Introduction to the Engineering of Rockets,* Wiley, New York, 1986.

[3]Anthony, T. C., Wie, B., and Carroll, S., "Pulse Modulated Control Synthesis for a Flexible Spacecraft," *Proceedings of the AIAA Guidance, Navigation, and Control Conference,* AIAA, Washington, DC, 1989, pp. 65–76.

[4]Kubiak, E. T., Penchuk, A. N., and Hattis, P. D., "A Frequency Domain Stability Analysis of a Phase Plane Control System," *Journal of Guidance, Control, and Dynamics,* Vol. 8, No. 1, 1985, pp. 50–55.

[5]Friedland, B., "Modeling Linear Systems for Pulsewidth-Modulated Control," *IEEE Transactions on Automatic Control,* Vol. AC-21, Oct. 1976, pp. 739–746.

[6]Friedland, B., *Control System Design: An Introduction to State-Space Methods,* McGraw-Hill, New York, 1987.

[7]Bernelli-Zazzera, F., Mantegazza, P., and Ongaro, F., "A Method to Design Structurally Constrained Discrete Suboptimal Control Laws for Actively Controlled Aircrafts," *Aerotecnica Missili e Spazio,* Vol. 67, No. 1-4, 1988, pp. 18–25.

[8]Wang, S. J., Lin, Y. H., and Ih, C. H. C., "Dynamics and Control of a Shuttle Attached Antenna Experiment," *Journal of Guidance, Control, and Dynamics,* Vol. 8, No. 3, 1985, pp. 344–353.

[9]Quinn, R. D., and Meirovitch, L., "Maneuver and Vibration Control of SCOLE," *Journal of Guidance, Control, and Dynamics,* Vol. 11, No. 6, 1988, pp. 542–553.

[10]Bernelli-Zazzera, F., Ercoli-Finzi, A., and Mantegazza, P., "Mixed Discrete/Pulse-Width Control of a Shuttle Attached Antenna," *Proceedings of the X Congresso Nazionale AIDAA,* ETS Editrice, Pisa, Italy, Oct. 1989, pp. 469–476.